0022-1767/79/1225-2032$02.00/0
THE JOURNAL OF IMMUNOLOGY

Vol. 122, No. 5, May 1979
Printed in U.S.A.

DETERMINATION OF THE NUMBER OF LYTIC SITES IN BICONCAVE AND SPHEROID ERYTHROCYTE GHOSTS AFTER COMPLEMENT LYSIS

JOHANN BAUER, ECKHARD R. PODACK, AND GUENTER VALET

From the Max-Planck-Institute fuer Biochemie, D-8033 Martinsried bei Muenchen, and the Scripps Clinic and Research Foundation, La Jolla, California 92037

C5b-9 binding to erythrocyte membranes was quantitated with the aid of C7-depleted serum, reconstituted with 125-J-C7. The number of C5b-9 complexes/cell was correlated with the transformation of ghosts from the biconcave to the spheroid shape by the combination of flow cytometry and sucrose density gradient ultracentrifugation. At low complement levels the mean number of C5b-9 complexes ranged from 300 to 1200 complexes/erythrocyte ghost, and biconcave as well as spheroid ghosts were found simultaneously in the same sample. The separation of both types of ghosts by sucrose density gradient centrifugation showed that the irreversible transition from the biconcave to the spheroid form occurred at a critical value of 850 C5b-9 complexes/erythrocyte ghost. Ghosts bearing less than 850 C5b-9 complexes were biconcave, and resealed ghosts bearing more than 850 C5b-9 complexes were spheroid and leaky. The spheroid transition is abrupt; no intermediate forms could be detected. The spheroid transformation is interpreted as a direct interaction between the C5b-9 complexes and membrane proteins resulting in a disturbance of the cytoskeleton of the erythrocyte ghost followed by spheroidization.

Cytolysis by complement (C) is effected by the C5b-9 complex which assembles after activation of C5 by the C5 convertase of the classical or the alternative pathway (1). The C5b-9 complex firmly binds to the cell membrane through hydrophobic interactions with the lipid bilayer (2, 3). C5b-9 binding to the target cell results in an increased ion flux across the membrane followed by swelling and rupture of the cell due to the protein osmotic pressure. Cell rupture is accompanied by release of intracellular protein.

Several concepts have been proposed as to the nature of the initial C lesion. Electron microscopical examination of C-lysed cells revealed the presence of membrane lesions that were interpreted as holes or pits in the membrane (4, 5). According to the doughnut hypothesis (6), the C5b-9 complex is inserted into the lipid bilayer of the membrane and forms transmembrane channels (7, 8). The mixed micelle hypothesis proposes the formation of "lipid channels" induced by the binding of membrane lipids to the C5b-9 complex and disturbance of the ordered bilayer structure (Podack, E. R., Biesecker, G., and Mueller-Eberhard, H. J., 1979. Proc. Natl. Acad. Sci. 76:897).

The structural lesion seen by electron microscopy has recently been identified as the membrane-bound C5b-9 complex (4, 9) in a dimeric state (Biesecker, G., Podack, E. R., Halverson, C., Mueller-Eberhard, H. J., 1979. J. Exp. Med. 149:448). It is not clear, however, whether this complex penetrates both halves of the lipid bilayer. Freeze fracture electron microscopy demonstrated the absence of C lesions on the cytoplasmic half of the bilayer (5). Together with conductance measurements across C-treated planar lipid bilayers (10) and steady state measurements of sucrose movements through C-treated cell membranes (11), these findings indicate a much smaller size of the C-induced transmembrane channel than seen by electron microscopy on negatively stained membranes or the isolated C5b-9 complex.

A new approach to the study of C-induced cell lysis was introduced by the application of flow cytometric techniques (12). With this method, one or several cell parameters (volume, fluorescence, absorption of light) can be simultaneously recorded at a rate of 800 to 1200 cells/sec. Thus, changes occurring on single cells can be correlated with the progress of C activation. Furthermore, this technique allows the correlation of C5b-9 binding to the cell membrane rupture, the size of membrane lesion at the moment of rupture, and the resealing behavior of C-lysed cells.

Recent observations by flow cytometry indicated that the transformation by C of erythrocytes from the biconcave to the spheroid form is of nonosmotic nature (12). The spheroid transformation probably is due to direct interaction of C5b-9 complex with erythrocyte membrane proteins responsible for the biconcave shape of the cell. It was also shown that the spheroid transformation of erythrocytes is accompanied by the loss of their ability to reseal (Bauer, J. and Valet, G., manuscript in preparation), whereas C-lysed biconcave cells were still osmotically responsive. These findings suggested that structural integrity is essential for the functional repair of C lesions. In the present study the number of C5b-9 complexes required for the spheroid transformation of biconcave cells is quantitated by measuring the uptake of radiolabeled C7 on biconcave and spheroid erythrocyte ghosts.

MATERIALS AND METHODS

Buffers. Veronal (2 mmoles/liter)-buffered saline (VBS), pH 7.4, low ionic strength buffer, obtained by 1 + 1 (v/v) dilution of VBS with 5% glucose solution (VBS-G), or by 1 + 1.5 dilution of VBS with 9.7% sucrose solution (VBS-S), and ethylenediamine-tetraacetic acid-containing buffer (VBS-EDTA), obtained by 4 + 1 dilution of VBS with a 0.1 mole/liter EDTA-

Received for publication November 14, 1978.
Accepted for publication February 13, 1979.
The costs of publication of this article were defrayed in part by the payment of page charges. This article must therefore be hereby marked *advertisement* in accordance with 18 U.S.C. Section 1734 solely to indicate this fact.

buffer were prepared with addition of 0.03% gelatin. The buffers were used without gelatin for cell counting in a Coulter counter or as sheath fluid in the flow cytometer. Except for VBS-EDTA, all buffers contained 0.15 mmoles/liter Ca^{++} and 1 mmole/liter Mg^{++} ions.

Erythrocytes. Sheep erythrocytes were prepared from fresh jugular vein blood, which was drawn into EDTA-coated polycarbonate tubes. The erythrocytes were optimally sensitized with rabbit-anti-sheep erythrocyte antiserum (Behringwerke, Marburg, Germany).

Complement components. C7 was isolated from human serum (13) and labeled with 125-J by the chloramin T method (14). One microgram C7 contained 1 μCi 125-J. C7-depleted human serum (2) was reconstituted with 40 μg 125-J-C7/ml serum. The lytic capacity of the reconstituted serum was 240 CH50/ml.

Lytic assay. Seventy microliters reconstituted C7-depleted serum were diluted with 180 μl VBS-G. Between 15 and 150 μl of this mixture (= 1 to 10 CH50) were incubated with 1×10^8 EA-cells at 37°C for 1 hr in a total volume of 250 μl VBS-G.

Lysis, radioactivity, and volume distribution measurements. Each assay was divided after the end of the incubation into three parts.

a) Fifty microliters of assay were diluted with 1 ml VBS-G and centrifuged for 2 min at 8000 × G. The degree of lysis was determined spectrophotometrically by measuring the hemoglobin in the supernatant at 412 nm.

b) One hundred fifty microliters of assay (= 6×10^7 cells) of the sample were layered on top of a 0.5-ml cushion of 10% sucrose solution sitting on top of a continuous 4.5-ml linear 30 to 60% sucrose density gradient. The cushion and the gradient contained uniformly 60 mmoles/liter NaCl and 2 mmoles/liter Veronal at pH 7.5. The gradient was centrifuged in a Beckman-Spinco L-50 ultracentrifuge (Beckman Instruments, Fullerton, Calif.) at 30,000 rpm (= 100,000 × G) with a SW 39 rotor for 1 hr at 0°C. After the end of the centrifugation, the gradient was divided into nine equal fractions. The radioactivity of each fraction was counted in a model A 511 001 Gamma spectrometer (Packard Instruments, Downers Grove, Ill.). The cell concentration in the fractions was determined with a Coulter model A electronic particle counter.

c) Fifty microliters of assay were used to measure the volume distribution curve of the cells by electric sizing with a Metricell flow cytometer (15) equipped with a cylindrical orifice of 65-μm diameter and 52-μm length. The particle beam was focused hydrodynamically through the center of the orifice. The cells were suspended in VBS-S buffer at 25°C (6.85 mSiemens), and between 800 to 1200 particles/sec were sized with an aperture current of 0.47 mA at a suction of 0.2 kg/cm^2.

Data analysis. The electrical volume pulse of each cell was amplified and stored according to the maximal pulse height in a 128 channel array of a 4096 step multichannel analyzer (Telefunken, Ulm, Germany). The volume distribution curves were plotted after the end of the measurement. The data were then transferred to a magnetic tape by an Interdata 74 computer (Interdata, Oceanport, N.J., 64 Kbyte core memory, 16 bit word length). The curves were further analyzed by optimally fitting logarithmic Gaussian normal distribution to the experimental curve (16).

RESULTS

The aim of the study was to determine the number of lytic sites on the biconcave and spheroid ghosts (12). For this purpose it was necessary to separate biconcave from spheroid ghosts and to count the radioactivity of specifically cell-bound 125-J-C7 as a marker for the number of lytic sites on the cell membrane of the separated cells.

Cell separation. Initial attempts to separate biconcave from spheroid ghosts by centrifugal elutriation (17) according to their different volumes were not successful, since the density of ghosts was too low to achieve good separations. The cells were separated, however, in a sucrose density gradient. On such gradients, advantage is taken of the different osmotic properties of biconcave and spheroid ghosts. Biconcave ghosts were resealed and osmotically responsive, since they did quantitatively shrink in hypertonic sucrose solutions (Bauer, J., Valet, G., manuscript in preparation). They remained on top of the gradient due to the low density of their intracellular content after the loss of hemoglobin. Spheroid ghosts, in contrast, were leaky and did not shrink in hypertonic sucrose solutions. The spheroid ghosts sedimented in the gradient, because the outside sucrose exchanged through the nonresealed lesions with the interior. Thus, permeable ghosts banded at the sucrose density corresponding to the density of their cell membrane. The following results were obtained with different doses of C: 90% of the cells incubated with 1 CH50 unit of C were biconcave (Fig. 1*a*) and 10% were spheroid. The 90% biconcave cells consist of 50% unlysed erythrocytes according to the result of the hemolytic assay and of 40% of biconcave ghosts. The unlysed erythrocytes and the lysed spheroid cells banded in the lower part of the gradient at a concentration around 50% sucrose after centrifugation (Fig. 1*b*). The biconcave ghosts were resealed and, therefore, remained in the upper part of the gradient at 30 to 35% sucrose concentration. After incubation with 3 CH50 units of C, more than 95% of the cells were lysed. The volume distribution curve was resolved by analysis into 66% biconcave and 34% spheroid ghosts (Fig. 1*c*). The biconcave ghosts remained on top of the gradient. They were well-separated from the permeable spheroid ghosts and the few intact cells that sedimented together in the lower part of the gradient (Fig. 1*d*). Ten CH50 units quantitatively lysed the erythrocytes. Only large cells were produced (Fig. 1*e*). They quantitatively banded in the lower part of the gradient (Fig. 1*f*) similarly to intact erythrocytes (Fig. 1*h*).

Number of lesions per cells. The number of cells and the radioactivity of each fraction were counted in order to enumerate the number of C5b-9 complexes per cell. The radioactivity values had to be corrected for free and unspecifically cell-bound 125-J-C7 of each fraction. Washing of the cells for removal of free and unspecifically bound radioactivity before gradient centrifugation was not possible since the volume distribution curve and the frequency distributions of the cells in the sucrose density gradient were altered by this procedure. The entire incubation mixture was, therefore, directly layered on top of the sucrose density gradient, and 125-J radioactivity and cell concentration were counted in all fractions after centrifugation. The free and unspecifically bound 125-J-C7 in each fraction was determined by centrifuging nonsensitized E-cells with 125-J-C7 containing serum into a separate sucrose density gradient as a control (Fig. 2). A linear decrease of unbound radioactivity from the top to the bottom of the gradient was found when the radioactivity of each fraction was plotted in percent of the total radioactivity on a logarithmic scale against the fraction number (Fig. 2). The linear decrease corresponds to the distribution of the free 125-J-C7 radioactivity in the gradient. The deviation from the line between fraction 2 to 5 is due to the unspecific adsorption of 125-J-C7 to the E-cells, which amounts to 1% of the total radioactivity. The specifically cell-bound 125-J-C7 was obtained by subtraction of the free and unspecifically cell-

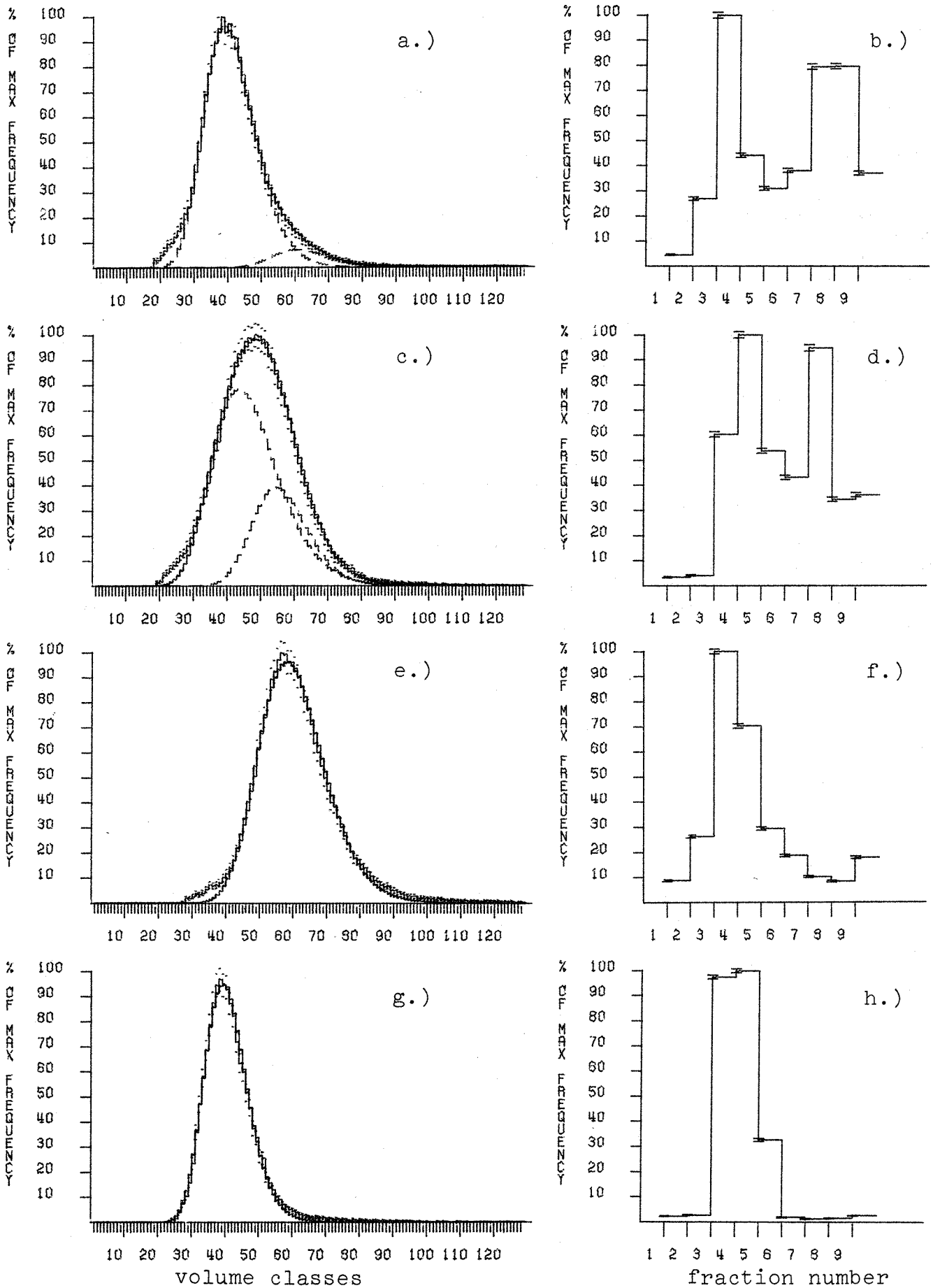
% OF MAX FREQUENCY
a.)
b.)
c.)
d.)
e.)
f.)
g.)
h.)
10 20 30 40 50 60 70 80 90 100 110 120
1 2 3 4 5 6 7 8 9
volume classes
fraction number

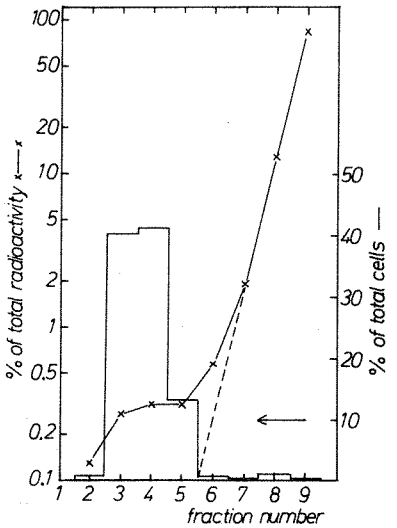

Figure 2. Distribution of radioactivity (×——×) and E-cells (——) in a 30–60% linear sucrose density gradient. Unsensitized E-cells were incubated with 125-J-C7 reconstituted, C7-depleted human serum and centrifuged as described under *Materials and Methods*. The direction of sedimentation was to the left, as indicated by the horizontal arrow. The free 125-J-C7 radioactivity decreases exponentially from the top to the bottom of the gradient. The deviation from the exponential decrease in fractions 2 to 5 is due to the unspecific adsorption of 125-J-C7 to the unlysed E-cells.

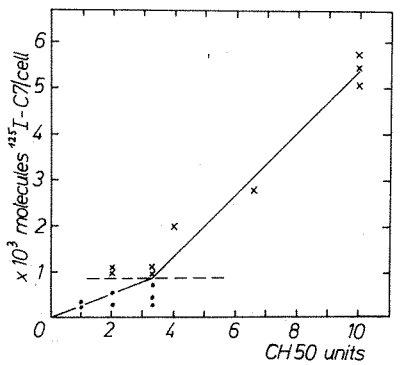

Figure 3. Specifically cell-bound 125-J-C7 molecules on sheep EA-cells *vs* the amount of C used for lysis. The biconcave (•) and spheroid (x) erythrocyte ghosts were separated after lysis by a 30–60% linear sucrose density gradient as shown in Figure 1. Erythrocyte ghosts below the dashed line (850 molecules 125-J-C7/cell) are always biconcave and above the line always spheroid. Both types of ghosts occur simultaneously in the assay when 2–3 CH50 units of C are used for lysis. Only spheroid ghosts are produced above 4 CH50 units.

bound 125-J-C7 of the control gradient (Fig. 2) from the total radioactivity of each gradient fraction. The number of cell-bound C7 molecules was calculated from the specifically cell-bound 125-J-C7 molecules assuming a m.w. of 120,000 Daltons (13) for C7. One cpm/10^7 cells correspond to 0.502 molecules cell-bound C7.

The following results were obtained from the analysis of the gradient fractions:

Intact E-cells centrifuged with 125-J-C7 containing C7-depleted serum, or unlysed EA-cells in lytic assays with 1 or 2 CH50 units C had between 125 and 150 molecules of unspecifically bound C7/cell.

Figure 3 and Table I summarize the result of several experiments that correlate the uptake of radiolabeled C7 with lysis and shape change of the erythrocytes. At low doses of C (2 to 3 CH50 units), biconcave ghosts and spheroid ghosts coexist simultaneously. The determination of the number of C5b-9 complexes on these two types of ghosts shows that biconcave ghosts bear less than 850 C5b-9 complexes/ghost, whereas spheroid ghosts invariably carry more than 850 C5b-9 complexes/ghost on their membrane. The average number of C5b-9 complexes/ghost can be calculated with the Poisson distribution $z = -ln\ (1 - y)$, where z is the number of complexes/cell and y the ratio of lysed cells. However, z is a statistical value and the actual number of complexes on individual cells may vary from the average value. This is demonstrated in Figure 3 for the dose range 1 to 3 CH50 units, where biconcave and spheroid ghosts with quite different numbers of lesions on their membrane are present in the same assay. The biconcave to spheroid transformation of the erythrocyte membrane occurs without noticeable statistical scatter and independently of the C dose as soon as the number of C5b-9 complexes/ghost exceeds the critical value of 850. The number of complexes/ghost by far exceeds this critical value at higher C doses (>4 CH50 units); therefore, only spheroid ghosts are seen in such assays.

TABLE I

Specificially bound C7 molecules/μM^2 cell surface after lysis of sheep erythrocytes with various C doses

Expt. No.	CH50 Units	Biconcave Ghosts	Spheroid Ghosts
1	1	5.73	
2	1	4.34	
3	1	4.32	
4	1	3.66	
5	2	9.69	19.72
6	2	5.06	19.75
7	3.3	8.53	18.00
8	3.3	13.80	20.29
9	4		37.14
10	6.6		51.89
11	10		108.34
12	10		102.78
13	10		94.90

Eight hundred fifty lesions/cell correspond to 16 lesions/μm^2 of cell surface. The area contribution of the C lesions to the total cell surface is 0.58% assuming a mean diameter of 215 Å (4, 5) for one C lesion.

DISCUSSION

The binding of C5b-9 complexes to erythrocyte membranes results in the osmotic lysis of the cell. Furthermore, the C5b-9

Figure 1. Volume distribution curves (*a, c, e, g*), and frequency distribution of EA-cells in 30–60% linear sucrose density gradients (*b, d, f, h*) after lysis with 1 CH50 (*a, b*), 3 CH50 (*c, d*), and 10 CH50 units (*e, f*) of 125-J-C7 containing C7-depleted human serum. Unlysed EA-cells (*g*) were centrifuged as a control (*h*). The direction of sedimentation was to the left, as indicated by the horizontal arrow (*b*). The volume distribution curves contain between 60,000 and 100,000 cells. The curves are normalized to their respective maximum and optimally fitted by one or two logarithmic Gaussian normal distributions (16). Ten percent, thirty-four percent, and one-hundred percent of the erythrocytes were spheroid ghosts after lysis with 1,3, and 10 CH50 units (50%, 95%, and 100% lysis) (*a, c, e*), whereas the remainder of cells were biconcave, similar to unlysed EA-cells (*g*). For the sucrose density gradients (*b, d, f, h*) the curves are normalized to the respective maximum of cell concentration. Cells (6×10^7) were applied per gradient. The gradient fractions 3 and 4 contain either intact erythrocytes (*h*), or spheroid ghosts (*f*), or a mixture of intact erythrocytes and spheroid ghosts (*b, d*). The resealed, osmotically responsive, biconcave ghosts were always located in fractions 6–8 (*b, d, f*).

complex effects a shape change of the erythrocyte ghost from the biconcave to the spheroid form which is independent of osmotic forces (12). It was also shown that the conversion of biconcave ghost to spheroid ghost is an all or nothing phenomenon; no intermediate forms could be demonstrated. We now show that the spheroid transformation occurs abruptly when the number of C5b-9 complexes/ghost approaches the critical value of 850. Under the experimental conditions used, this value represents the upper limit, since the limiting component was C7. All EAC1-7 sites are converted to EAC1-9 sites in the presence of excess C8 and C9. Thus the attachment of 850 C5b-9 complexes/cell has a dramatic effect on the shape of the cell.

It is known that the C5b-9 complex interacts primarily with the lipid part of the membrane and that isolated C5b-9 complexes bind 1400 lecithin molecules/C5b-9 dimer (E. R. Podack, G. Biesecker, and H. J. Mueller-Eberhard, 1979. Proc. Natl. Acad. Sci. 76:897). Nevertheless, it appears unlikely that the shape change is induced solely by interaction with membrane lipids since 850 complexes/ghost would affect only 1% of the total lipids. In line with this argument is the hypothesis that the biconcave shape of the erythrocyte is maintained by the cytoskeleton composed of transmembrane proteins and the spectrin layer at the inner side of the cell membrane (18–20), rather than by the lipid part of the membrane. It is conceivable that the interaction of the C5b-9 complex in the plane of the membrane with membrane protein results in their loss of attachment to the spectrin layer. The cell membrane subsequently changes its shape due to the surface tension of the lipid bilayer. This interpretation envisions that the disturbance of a few attachment points of spectrin is sufficient to release the cell into its thermodynamically favored spheroid form.

Direct interaction of the C5b-9 complex with membrane proteins may also be responsible for the stability of the C5b-9 complex in erythrocyte membranes which is in contrast to C5b-9 complexes in artificial lipid bilayers devoid of integral membrane proteins. In the latter case the C5b-9 complexes are easily released from the bilayer lipid as indicated by C-induced phospholipid release from liposomes (21) and as demonstrated directly by the formation of mixed micelles between phospholipid and C5b-9-protein (Podack, E. R., Biesecker, G., and Mueller-Eberhard, H. J., 1979. Proc. Natl. Acad. Sci. 76:897). The proposed hypothesis of a direct interaction between C5b-9 and erythrocyte membrane proteins will be subjected to further experiments.

REFERENCES

1. Podack, E. R., W. P. Kolb, and H. J. Mueller-Eberhard. 1976. The C5b-9 complex: subunit composition of the classical and alternative pathway generated complex. J. Immunol. 116:1431.
2. Podack, E. R., W. P. Kolb, and H. J. Mueller-Eberhard. 1978. The C5b-9 complex: formation, isolation, and inhibition of its activity by lipoprotein and the S-protein of human serum. J. Immunol. 120: 1841.
3. Podack, E. R., and H. J. Mueller-Eberhard. 1978. Binding of desoxycholate, phosphatidylcholine vesicles, lipoprotein and S-protein to the terminal complexes C5b-6, C5b-7, and C5b-8 and C5b-9. J. Immunol. 121:1025.
4. Tranum-Jensen, J., S. Bhakdi, B. Bhakdi-Lehnen, O. J. Bjerrum, and V. Speth. 1978. Complement lysis: the ultrastructure and orientation of the C5b-9 complex on target sheep erythrocyte membranes. Scand. J. Immunol. 7:45.
5. Seeman, P., and G. H. Iles. 1973. Pits in the freeze-cleavage plane of normal erythrocyte membranes, and ultrastructure of membrane lesions in immune lysis. *In* The Red Blood Cell. Springer-Verlag, New York. Pp. 169–180.
6. Mayer, M. M. 1972. Mechanism of cytolysis by complement. Proc. Natl. Acad. Sci. 69:2954.
7. Hammer, C. H., M. L. Shin, A. S. Abramovitz, and M. M. Mayer. 1977. On the mechanism of cell membrane damage by complement: evidence on insertion of polypeptide chains from C8 and C9 into the lipid bilayer of erythrocytes. J. Immunol. 119:1.
8. Boyle, M. D. P., J. J. Langone, and T. Borsos. 1978. Studies on the terminal stages of immune hemolysis. J. Immunol. 120:1721.
9. Podack, E. R., C. Halverson, A. F. Esser, W. P. Kolb, and H. J. Mueller-Eberhard. 1978. Regeneration of the ability to interact with lipid by selective removal of the S-protein. J. Immunol. 121: 1025.
10. Michaels, D. W., A. S. Abramovitz, C. H. Hammer, and M. M. Mayer. 1976. Increased ion permeability of planar lipid bilayer membranes after treatment with C5b-9 cytolytic attack mechanism of complement. Proc. Natl. Acad. Sci. 73:2852.
11. Sims, P. J., and P. K. Lauf. 1978. Steady state analysis of tracer exchange across the C5b-9 complement lesion in a biological membrane. Proc. Natl. Acad. Sci. In press.
12. Valet, G., and W. Opferkuch. 1975. Mechanism of complement-induced cell lysis: demonstration of a three-step mechanism of EAC1-8 cell lysis by C9 and of a non osmotic swelling of erythrocytes. J. Immunol. 115:1028.
13. Podack, E. R., W. P. Kolb, and H. J. Mueller-Eberhard. 1976. Purification of the sixth and seventh component of human complement without loss of hemolytic activity. J. Immunol. 116:263.
14. Mc Conahey, P. J., and F. J. Dixon. 1976. A method of trace iodination of proteins for immunologic studies. Int. Arch. Allergy Appl. Immunol. 29:185.
15. Kachel, V. 1976. Basic principles of electrical sizing of cells and particles and their realization in the new instrument "Metricell". J. Histochem. Cytochem. 24:211.
16. Valet, G., H. Hofmann, and G. Ruhenstroth-Bauer. 1976. The computer analysis of volume distribution curves: demonstration of two erythrocyte populations of different size in the young guinea pig and analysis of the mechanism of immune lysis of cells by antibody and complement. J. Histochem. Cytochem. 24:231.
17. Meistrich, M. L. 1977. Separation of spermatogenic cells and nuclei from rodent testes. Methods Cell Biol. 15:15.
18. Gomperts, B. 1977. The plasma membrane: models for structure and function. *In* The Red Cell Membrane. Academic Press, Inc., London. Pp. 97–107.
19. Weinstein, R. S. 1974. Morphology of adult red cells. *In* The Red Blood Cell. Springer-Verlay, New York. Pp. 213–268.
20. Hainfield, Y. J., and Th. L. Steck. 1977. The submembrane reticulum of the human erythrocyte: a scanning electron microscope study. J. Supramol. Struct. 6:301.
21. Shin, M. L., W. A. Paznekas, and M. M. Mayer. 1978. Mechanism of membrane damage by complement-effect of length and unsaturation of acyl chains in liposomal bilayers and effect of cholesterin concentration in sheep erythrocyte and liposomal membranes. J. Immunol. 120:1996.